

Theory of tunneling magnetoresistance of an epitaxial Fe/MgO/Fe(001) junction

J. Mathon and A. Umerski

Department of Mathematics, City University, London EC1V 0HB, United Kingdom

(Received 21 December 2000; published 10 May 2001)

Calculation of the tunneling magnetoresistance (TMR) of an epitaxial Fe/MgO/Fe(001) junction is reported. The conductances of the junction in its ferromagnetic and antiferromagnetic configurations are determined without any approximations from the real-space Kubo formula using tight-binding bands fitted to an *ab initio* band structure of iron and MgO. The calculated optimistic TMR ratio is in excess of 1000% for an MgO barrier of ≈ 20 atomic planes and the spin polarization of the tunneling current is positive for all MgO thicknesses. It is also found that spin-dependent tunneling in an Fe/MgO/Fe(001) junction is not entirely determined by states at the Γ point ($\mathbf{k}_{\parallel}=0$) even for MgO thicknesses as large as ≈ 20 atomic planes. All these results are explained qualitatively in terms of the Fe majority- and minority-spin surface spectral densities and the complex MgO Fermi surface.

DOI: 10.1103/PhysRevB.63.220403

PACS number(s): 75.70.Cn, 75.45.+j

The conductance $\Gamma(H_s)$ of a tunnel junction in an applied saturating field H_s is much higher than $\Gamma(0)$ in zero field when the electrode magnetizations are antiparallel.¹⁻³ The effect is called tunneling magnetoresistance (TMR) and the change in the conductance relative to $\Gamma(0)$ (optimistic TMR ratio) can be as high as 50%. Such high TMR ratios are achieved for iron, cobalt, or permalloy electrodes, and an Al₂O₃ barrier, which is amorphous. An amorphous barrier makes a rigorous calculation of the TMR virtually impossible since the electron momentum parallel to the barrier \mathbf{k}_{\parallel} is not conserved. On the other hand, when \mathbf{k}_{\parallel} is conserved (coherent tunneling), the conductance of a tunneling junction can be evaluated quite rigorously from the Kubo formula.⁴ The Kubo formula has already been applied to a cobalt junction with a vacuum gap^{4,5} but little theoretical progress has been made for junctions with an insulating barrier since junctions for which tunneling could be regarded as coherent were lacking. A notable exception is the calculation of MacLaren *et al.*⁶ for an Fe junction with a ZnSe semiconductor spacer. The situation has changed radically with the recent demonstration^{7,8} of tunneling in an epitaxial Fe/MgO/Fe(001) junction. To the first approximation (neglecting defects), tunneling should be coherent and Fe/MgO/Fe(001) is, therefore, an ideal system to be studied theoretically.

We report here our calculation of the TMR for an epitaxial Fe/MgO/Fe(001) junction. It will be shown that, given a fully realistic band structure of the Fe electrodes and MgO barrier, the tunneling conductance can be evaluated from the Kubo formula without any approximations. The Kubo formula itself is, of course, exact in the low-bias (linear-response) regime.

Our principal results are that the calculated optimistic TMR ratio is very large, in excess of 1000% for an MgO barrier of ≈ 20 atomic planes, and the spin polarization of the tunneling current is positive (as in junctions based on an Al₂O₃ barrier). We also find that spin-dependent tunneling in an Fe/MgO/Fe(001) junction is not entirely determined by states at the Γ point ($\mathbf{k}_{\parallel}=0$) even for MgO thicknesses as large as ≈ 20 atomic planes.

It is known experimentally⁹ that thin epitaxial bcc Fe(001) films grow pseudomorphically on a rocksalt MgO(001) sub-

strate so that the Fe atoms sit above the O ions. The Fe lattice is, therefore, rotated by 45° relative to the MgO lattice. Low-energy electron-diffraction studies¹⁰ show that the Fe-O distance is almost exactly equal to the distance between the neighboring MgO atomic planes. This picture is confirmed by first-principle calculations of Li and Freeman.¹¹ There is only a small lattice mismatch of about 3.5% between the Fe-Fe and O-O in-plane distances. Li and Freeman¹¹ further show that the electron population at the MgO interface plane is virtually the same as for the clean MgO surface and the Fe interface plane also behaves like a free Fe surface.

Based on these results, we neglect the small lattice mismatch between Fe and MgO and assume that the whole Fe/MgO/Fe(001) junction grows epitaxially. We describe the band structure of the electrodes by tight-binding bands fitted to the *ab initio* band structure of bcc Fe (Ref. 12) and that of the barrier by tight-binding bands fitted to the band structure of bulk MgO.¹³ The on-site potentials in the Fe interface plane were adjusted self-consistently to reproduce the correct surface moment of Fe.¹¹ No adjustments of the surface potentials of MgO were found to be necessary. Hoppings up to third-nearest neighbors were used. The band gap for the band structure of bulk MgO we use is 7.6 eV, which is in a good agreement with the height of the tunneling barrier of 3.6 eV obtained by Wulfhekel *et al.*⁷ The fact that the observed tunneling barrier is about half of the band gap suggests that the Fermi level of the junction lies close to the middle of the gap. This is in very good agreement with the calculated results of Li and Freeman¹¹ who place the Fermi level 3.5 eV above the top of the valence band of MgO. We have, therefore, used this value to align our tight-binding bands of Fe and MgO. Finally, the tight-binding hopping integrals between Fe and MgO were determined by Harrison's method.¹⁴

We work in a mixed representation that is Bloch-like in the direction parallel to the layers and atomiclike in the perpendicular direction. Using this representation, one can readily express the current matrix elements in the real-space Kubo formula¹⁵ in terms of one-electron Green's functions at the Fermi surface ($E=E_F$). It is then easy to show^{4,5} that the total conductance Γ^σ in a spin channel σ is given by

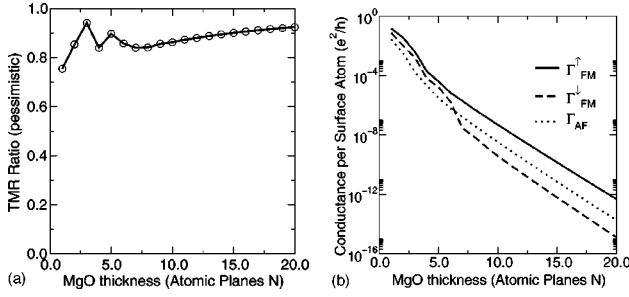


FIG. 1. (a) Dependence of the pessimistic TMR ratio R_{TMR} of an Fe/MgO/Fe(001) junction on MgO thickness. (b) Dependencies of the total conductances Γ_{FM}^{\uparrow} , Γ_{FM}^{\downarrow} , and Γ_{AF} on MgO thickness.

$$\Gamma^{\sigma} = \frac{4e^2}{h} \sum_{\mathbf{k}_{\parallel}} \text{Tr}([\mathbf{T}_{\sigma} \text{Im} \mathbf{G}_0^{\sigma}(\mathbf{k}_{\parallel})] \cdot [\mathbf{T}_{\sigma}^{\dagger} \text{Im} \mathbf{G}_1^{\sigma}(\mathbf{k}_{\parallel})]), \quad (1)$$

where 0 and 1 are any two neighboring atomic planes in the junction, the summation is over the two-dimensional Brillouin zone, and the trace is over the orbital indices corresponding to s, p, d orbitals that are required in a tight-binding parametrization of the junction. Finally, $\mathbf{G}_0^{\sigma}(\mathbf{k}_{\parallel})$, $\mathbf{G}_1^{\sigma}(\mathbf{k}_{\parallel})$ are the one-electron Green's functions at the left (right) surfaces of a junction that is separated into two independent parts by an imaginary cleavage plane drawn between the atomic planes 0, 1. The separation of the junction into two independent parts is made simply for calculational purposes. The junction remains physically connected and the interaction between the left and right parts is fully restored in Eq. (1) by the matrices \mathbf{T}_{σ} and $\mathbf{T}_{\sigma}^{\dagger}$ defined by

$$\mathbf{T}_{\sigma} = \mathbf{t}_{01}(\mathbf{k}_{\parallel}) [\mathbf{I} - \mathbf{G}_1^{\sigma}(\mathbf{k}_{\parallel}) \mathbf{t}_{01}^{\dagger}(\mathbf{k}_{\parallel}) \mathbf{G}_0^{\sigma}(\mathbf{k}_{\parallel}) \mathbf{t}_{01}(\mathbf{k}_{\parallel})]^{-1}, \quad (2)$$

where \mathbf{I} is a unit matrix in the orbital space and $\mathbf{t}_{01}(\mathbf{k}_{\parallel})$ is the tight-binding hopping matrix connecting the surfaces 0 and 1.

Equation (1) is the computationally most efficient way of calculating the conductance since only the diagonal (in the plane index i) elements of the left and right surface Green's functions of the cut junction are required. The surface Green's functions \mathbf{G}_0^{σ} , \mathbf{G}_1^{σ} are determined from the surface Green's function \mathbf{G}_s of a semi-infinite Fe electrode using the Dyson equation. \mathbf{G}_s itself is calculated by the generalized

Möbius transformation method,¹⁶ which allows us to determine \mathbf{G}_s quite accurately for an imaginary part of the energy ϵ as small as 10^{-12} Ry.

The numerical evaluation of Eq. (1) for a tunneling junction is not straightforward. The exact Green's function in the MgO barrier should decay exponentially. However, a small imaginary part ϵ of the energy results in a propagating component, which leads to a spurious “metalliclike” ballistic conductance independent of the barrier thickness. For a thick barrier, this spurious contribution eventually becomes dominant for any nonzero ϵ . This problem can be eliminated by reformulating Eq. (1) in terms of the off-diagonal elements of the Green's function connecting the surfaces of the left and right electrodes.¹⁷ However, it is computationally more demanding to calculate the off-diagonal components of the Green's function than the diagonal ones in Eq. (1).

The second problem is that the partial conductance $\Gamma^{\sigma}(\mathbf{k}_{\parallel})$ exhibits very sharp peaks in certain regions of the two-dimensional Brillouin zone (2D BZ). Since such peaks make a significant contribution to the total conductance, an extremely fine mesh of \mathbf{k}_{\parallel} points is required. We find that up to $\approx 10^6$ \mathbf{k}_{\parallel} points in the irreducible segment of the 2D BZ are needed to achieve convergence. Moreover, with a fine mesh of \mathbf{k}_{\parallel} points one also needs a very small ϵ for numerical stability.

Given the requirement of a very fine mesh of \mathbf{k}_{\parallel} points, it is best to use the computationally most efficient Eq. (1). To minimize the effect of a finite ϵ (10^{-12} Ry), we calculate the conductances by cutting the junction in the middle of the MgO barrier. The most stringent test that the error due to a finite ϵ is negligible is to check that all the conductances decrease exponentially in the limit of a thick barrier. This is satisfied in our calculations for MgO barriers as thick as 20 atomic planes.

We are now ready to discuss our results. We use the (pessimistic) tunneling magnetoresistance ratio $R_{TMR} = [\Gamma(H_s) - \Gamma(0)]/\Gamma(H_s)$. The dependence of R_{TMR} on the thickness of the MgO barrier is shown in Fig. 1(a). The majority-spin Γ_{FM}^{\uparrow} and minority-spin Γ_{FM}^{\downarrow} conductances in the ferromagnetic configuration of the junction and the conductance Γ_{AF} of electrons of either spin in the antiferromagnetic configuration are plotted against the MgO thickness on a logarithmic scale in Fig. 1(b). The TMR ratio oscillates initially with

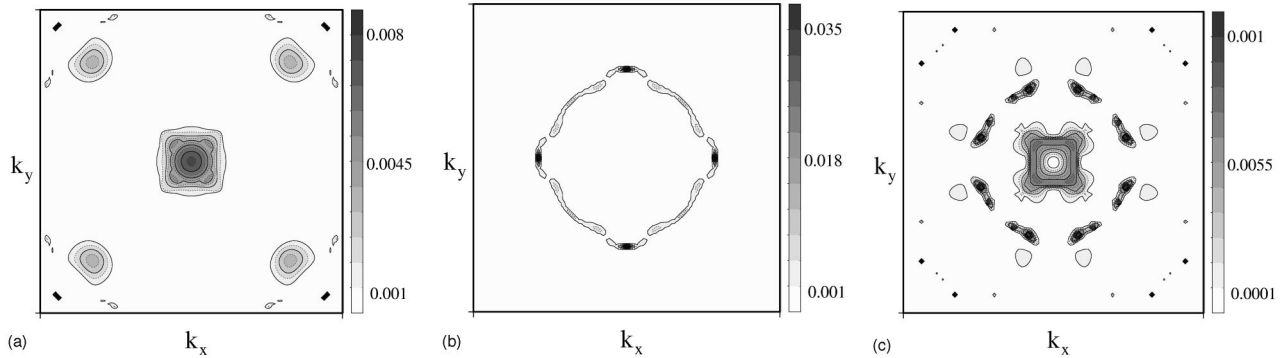


FIG. 2. Distribution of the partial conductances in the two-dimensional Brillouin zone for an Fe/MgO/Fe(001) junction with four atomic planes of MgO: (a) $\Gamma_{FM}^{\uparrow}(\mathbf{k}_{\parallel})$, (b) $\Gamma_{FM}^{\downarrow}(\mathbf{k}_{\parallel})$, and (c) $\Gamma_{AF}(\mathbf{k}_{\parallel})$.

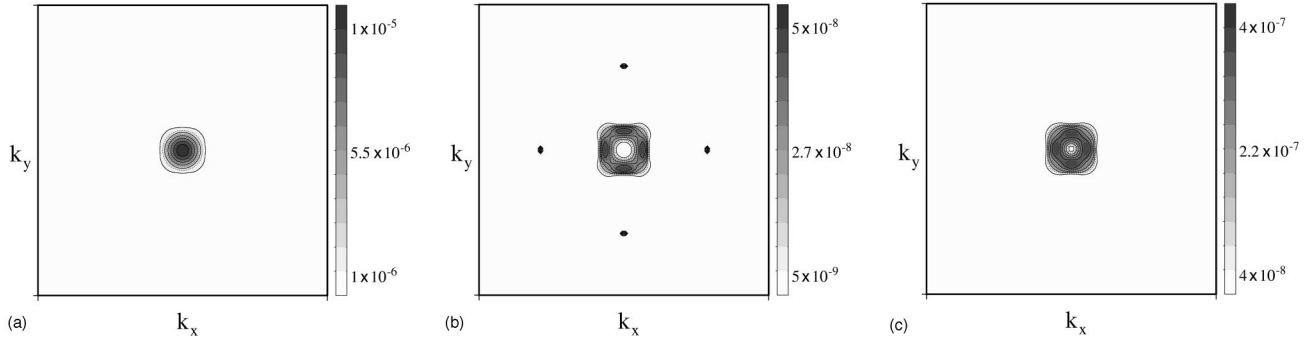


FIG. 3. Distribution of the partial conductances in the two-dimensional Brillouin zone for an Fe/MgO/Fe(001) junction with eight atomic planes of MgO: (a) $\Gamma_{FM}^\uparrow(\mathbf{k}_\parallel)$, (b) $\Gamma_{FM}^\downarrow(\mathbf{k}_\parallel)$, and (c) $\Gamma_{AF}(\mathbf{k}_\parallel)$.

MgO thickness but after about seven atomic planes of MgO, it stabilizes and increases only slowly reaching a very high value of 0.92 for 20 atomic planes of MgO. This corresponds to the optimistic ratio of some 1200%. The behavior of the individual conductances is more informative. First, it is clear from Fig. 1(b) that the majority-spin conductance is always higher than the minority-spin conductance. It follows that the calculated spin polarization of the tunneling current is positive, as found experimentally for junctions based on an Al_2O_3 barrier. It is also clear that after some ten atomic planes of MgO the junction reaches an asymptotic regime with all the conductances decreasing exponentially with MgO thickness. However, the slope of Γ_{FM}^\uparrow is somewhat smaller than that of Γ_{FM}^\downarrow and Γ_{AF} . This indicates that even for 20 atomic planes of MgO, the decay of the conductances in these three channels is not controlled by the same exponential factor.

To clarify the rather unusual behavior of the Fe/MgO/Fe junction, we show in Figs. 2 and 3 the \mathbf{k}_\parallel dependence of the partial conductances $\Gamma_{FM}^\sigma(\mathbf{k}_\parallel)$ and $\Gamma_{AF}(\mathbf{k}_\parallel)$ in the 2D BZ. The results shown in Fig. 2 are for four atomic planes of MgO and those in Fig. 3 for ten planes. These thicknesses were chosen because they correspond to the transition from a preasymptotic regime to the asymptotic regime discussed above.

We begin with Fig. 2. The conductance Γ_{FM}^\uparrow shown in Fig. 2(a) has the expected maximum at $\mathbf{k}_\parallel=0$ but also at four

subsidiary maxima along the $k_x=k_y$ lines in the 2D BZ. On the other hand, Γ_{FM}^\downarrow [Fig. 2(b)] is virtually zero at the Γ point and most conduction goes through a ‘‘ring’’ well removed from $\mathbf{k}_\parallel=0$. Finally, Γ_{AF} [Fig. 2(c)] has maxima along two concentric ‘‘rings’’ in the 2D BZ but a minimum at $\mathbf{k}_\parallel=0$. For a thicker MgO barrier (ten atomic planes), the junction moves closer to the expected asymptotic regime. The conductance Γ_{FM}^\uparrow [Fig. 3(a)] is now dominated by the Γ point. Similarly, Γ_{AF} [Fig. 3(c)] and Γ_{FM}^\downarrow [Fig. 3(b)] are determined by the inner ‘‘ring’’ that is also very close to the Γ point. However, both the conductances Γ_{AF} and Γ_{FM}^\downarrow have a minimum at the Γ point.

The calculated dependence of the TMR on the thickness of MgO can be understood qualitatively in terms of the surface spectral densities $(-1/\pi)\text{Im} \mathbf{G}_s^\sigma(E_F, \mathbf{k}_\parallel)$ of Fe(001) and the complex Fermi surface (FS) of MgO. They are reproduced in Fig. 4. We first show in Fig. 4a the smallest decay constant $\text{Im} k_\perp(\mathbf{k}_\parallel)$ for electrons in the MgO barrier (the lowest sheet of the complex MgO FS). Perpendicular tunneling $\mathbf{k}_\parallel=0$ is clearly favored but there are four subsidiary minima of $\text{Im} k_\perp(\mathbf{k}_\parallel)$ along the $k_x=k_y$ lines. These are responsible for the four subsidiary maxima of Γ_{FM}^\uparrow seen in Fig. 2(a). The other factor contributing to the maxima is that the surface spectral density of the majority-spin electrons [Fig. 4(b)] is distributed over the whole 2D BZ. On the other hand, the spectral density of the minority-spin electrons [Fig. 4(c)] is

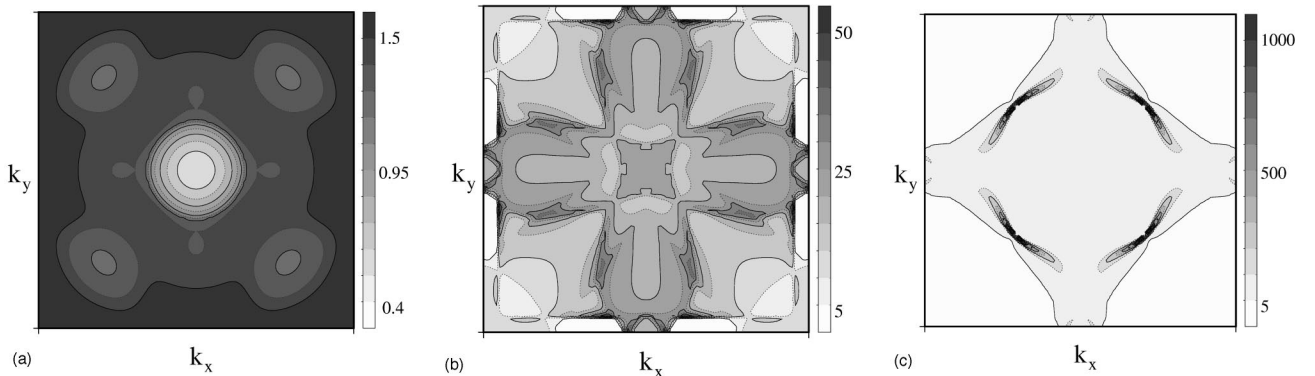


FIG. 4. (a) The smallest decay constant $\text{Im} k_\perp(\mathbf{k}_\parallel)$ of electrons in the MgO barrier (the lowest sheet of the complex MgO Fermi surface). (b) The majority-spin surface spectral density of Fe(001). (c) The minority-spin surface spectral density of Fe(001).

concentrated along the large ring seen already in Fig. 2(b) and there is hardly any density at the Γ point. This factor alone explains the behavior of Γ_{FM}^{\downarrow} seen in Fig. 2. The behavior of Γ_{AF} is determined by a superposition of the pictures for the \uparrow - and \downarrow -spin spectral densities. As the thickness of MgO increases, the contributions from the parts of the 2D BZ further away from the Γ point are weakened, and that explains the transition of the junction from the preasymptotic to the asymptotic regime.

It remains to be clarified why the MgO junction does not reach the expected asymptotic regime in which all the conductances decay with the same $\text{Im } k_{\perp}(\mathbf{k}_{\parallel}=0)$ (perpendicular tunneling). Figure 3 shows that there is virtually no tunneling at the Γ point in the minority-spin channel and that explains why $\Gamma_{AF}(\mathbf{k}_{\parallel})$ and $\Gamma_{FM}^{\downarrow}(\mathbf{k}_{\parallel})$ decay faster with MgO thickness than Γ_{FM}^{\uparrow} . Neither the minority-spin spectral density nor the MgO complex FS can explain the presence of a “hole” in the conductances $\Gamma_{AF}(\mathbf{k}_{\parallel})$ and $\Gamma_{FM}^{\downarrow}(\mathbf{k}_{\parallel})$ at the Γ point. We, therefore, conclude that hopping of minority-spin electrons from Fe to MgO is forbidden at the Γ point. This is supported by the fact that the “hole” in question is present at all thicknesses of MgO (see Figs. 2 and 3).

It is clear from Figs. 3 and 4 that the calculated large TMR ratio R_{TMR} in the asymptotic regime is due, entirely, to a very low spectral density of minority-spin electrons at the Γ point. To observe such a large R_{TMR} it is, therefore, essential that the Fe/MgO interface is perfect so that the theoretical minority-spin spectral density is well reproduced. The behavior of R_{TMR} at small thicknesses of MgO is determined by large peaks of the spectral density (hot spots) located outside the Γ point. These are very sensitive not only to interfacial roughness but also to the symmetry of the junction. Our results show that when the on-site potentials of one of the Fe electrodes are shifted slightly away from their nominal values, the TMR ratio can be altered very significantly in the preasymptotic regime. However, the calculated values of R_{TMR} remain very stable for MgO thicknesses greater than seven or eight atomic planes. We, therefore,

conclude that the optimum MgO thickness for observation of a large TMR ratio in an Fe/MgO/Fe(001) junction is around ten atomic planes of MgO.

Finally, we compare our results with those for an Fe/ZnSe/Fe junction.⁶ First, the conductances for an Fe/MgO/Fe junction are a factor of 10^8 smaller than those for Fe/ZnSe/Fe. This is because the band gap of Mg is 7.6 eV whereas the calculated gap⁶ for ZnSe is only 1.34 eV. Despite this, the qualitative dependencies of the conductances Γ_{FM}^{\uparrow} , Γ_{FM}^{\downarrow} , and Γ_{AF} on barrier thickness are strikingly similar. In particular, the “ring”-shaped feature in Γ_{FM}^{\downarrow} is also found by MacLaren *et al.*⁶ for a small thickness of ZnSe. We attribute it to the corresponding feature in the Fe surface spectral density [Fig. 4(c)]. The majority conductances for a thin barrier are different for MgO and ZnSe. This is most likely due to interfacial states⁶ that dominate the conductance in these channels when the band gap is small (as in ZnSe) and the barrier is thin. For a thick barrier, our interpretation based on the Fe surface spectral density and barrier complex Fermi surface should be valid for any rocksalt and tetrahedral *s-p* bonded barriers since their bulk band structures are similar. Apart from the magnitude, the results for MgO and ZnSe are, therefore, very similar in this asymptotic limit. For the same reason, the “hole” in the minority-spin channel at the Γ point is common to MgO and ZnSe. The method of MacLaren *et al.*,⁶ based on matching wave functions across the barrier, shows unambiguously that the “hole” is due to a symmetry mismatch of the wave functions. The spin polarization of the tunneling current is positive both for MgO and ZnSe barriers. We believe this is due to a slower decay of the wave functions of *s-p* electrons in the barrier, which thus dominate tunneling, combined with the fact that the polarization of *s-p* electrons in Fe is opposite to that of the *d* electrons (magnetization).

We are grateful to D.M. Edwards, M.A. Villeret, and B. Heinrich for helpful discussions. The support of the Engineering and Physical Sciences Research Council (EPSRC UK) under Grant No. GR/L92945 is gratefully acknowledged.

¹T. Miyazaki and N. Tezuka, *J. Magn. Magn. Mater.* **139**, L231 (1995).

²J.S. Moodera, L.R. Kinder, T.M. Wong, and R. Meservey, *Phys. Rev. Lett.* **74**, 3273 (1995).

³Y. Li, X.W. Li, G. Xiao, R.A. Altman, W.J. Gallagher, A. Marley, K. Roche, and S.S.P. Parkin, *J. Appl. Phys.* **83**, 6515 (1998).

⁴J. Mathon, *Phys. Rev. B* **56**, 11 810 (1997).

⁵J. Mathon and A. Umerski, *Phys. Rev. B* **60**, 1117 (1999).

⁶J.M. MacLaren, X.-G. Zhang, W.H. Butler, and X. Wang, *Phys. Rev. B* **59**, 5470 (1999).

⁷W. Wulfhekel, M. Klaua, D. Ullmann, F. Zavaliche, J. Kirschner, R. Urban, T. Monchesky, and B. Heinrich, *Appl. Phys. Lett.* **78**, 509 (2001).

⁸S.S.P. Parkin (unpublished); M. Bowen, V. Cros, F. Petroff, A. Fert, C. Martinez Boubeta, J.L. Costa-Kramer, J.V. Anguita, A. Cebollada, F. Briones, J.M. de Teresa, L. Morellon, M.R. Ibarra,

F. Guell, F. Peiro, and A. Cornet (unpublished).

⁹T. Kanaji, T. Kagotani, and S. Nagata, *Thin Solid Films* **32**, 217 (1976).

¹⁰T. Urano and T. Kanaji, *J. Phys. Soc. Jpn.* **57**, 3043 (1988).

¹¹Chun Li and A.J. Freeman, *Phys. Rev. B* **43**, 780 (1991).

¹²D.A. Papaconstantopoulos, *Handbook of the Band Structure of Elemental Solids* (Plenum, New York, 1986).

¹³Ven-chung Lee and How-sen Wong, *J. Phys. Soc. Jpn.* **45**, 895 (1978).

¹⁴W.A. Harrison, *Solid State Theory* (Dover, New York, 1979).

¹⁵J. Mathon, A. Umerski, and M.A. Villeret, *Phys. Rev. B* **55**, 14 378 (1997).

¹⁶A. Umerski, *Phys. Rev. B* **55**, 5266 (1997).

¹⁷C. Caroli, R. Combescot, P. Nozieres, and D. Saint-James, *J. Phys. C* **4**, 916 (1971).